ADVANCED MATERIALS

DOI: 10.1002/adma.200602709

Engineered Microcapsules Fabricated from Reconstituted Spider Silk**

By *Kevin D. Hermanson*, *Daniel Huemmerich, Thomas Scheibel*,* and *Andreas R. Bausch**

In applications such as flavor encapsulation, drug delivery, and biomedical devices, microencapsulation is developing into an increasingly effective method for the protection and delivery of active ingredients. Herein, we show that spider-silk proteins are well-suited for producing responsive microcapsules with high mechanical stability. Emulsion interfaces are harnessed to induce the controlled self-assembly of these proteins into predominantly β-sheet configurations, resulting in a mechanically stable thin polymer shell. Capsules transferred into a continuous phase can readily encapsulate large molecules, while allowing small molecules to permeate freely. The capsules demonstrate good chemical stability, which is attributed to the β-sheet-rich structure of the self-assembled spider-silk proteins. These microcapsules represent a new class of biomimetic materials, exhibiting functionalities that can be further modified and controlled on the molecular level.

A major challenge in creating efficacious devices for microencapsulation of a broad class of active ingredients is the necessity to provide a variety of functionalities for different applications. For some applications even multifunctionality is highly desirable. Microcapsules used for bioprocesses not only have to protect the ingredients from the surrounding environment and release them in a controlled manner; they must also not induce an immunological or allergenic response in the respective host. To perform these different functions, an ideal microcapsule has to be fabricated from a material that is strong, biocompatible, and easily functionalized. To date most encapsulation techniques have made use of synthetic polymers, inorganic materials, or colloidal particles.[1–10] However, self-assembly of biomolecules would enable the simultaneous use of many more functionalities, especially those that are of interest for biomedical applications. Strategies that use amphiphilic short peptides are already very promising for building new nanostructured materials with novel functional properties;[5–7,10–15] however, larger protein molecules represent a more controllable and functionalizable material, which can be designed to respond to external triggers such as pH and temperature,[16–19] bind to cells or enzymes,[20] and degrade when exposed to specific proteases.[21]

Building microencapsulation devices based on proteins is challenging because the protein's self-assembly must be precisely controlled. One approach that has been used previously to form peptide-based microcapsule devices is to use small amphiphilic polypeptides and proteins (6 to 100 residues) to form vesicles.[5–7,10] However, this self-assembly approach does not necessarily work for larger proteins (e.g., exceeding a molecular weight of 10 kDa ($1\ \mathrm{Da} = 1.660 \times 10^{-27}$ kg)), which have the important advantage that more functionalities, such as effector molecules or recognition sites, can be incorporated. Another approach that has been used for such large proteins is to electrostatically adsorb a protein onto an emulsion droplet that has a charged surfactant at the surface, or to a charged solid template.[8,22,23] Because this approach is dependant on protein charge, it is sensitive to pH changes in the surrounding environment. A more versatile approach to microcapsule formation would be to template a liquid surface with a functional self-assembling protein that is able to capture the templated shape by noncovalent or covalent bonds. This approach would be less sensitive to environmental conditions and only require one adsorbing species. In Nature, self-assembly of molecules such as DNA and proteins is a common feature, and one prerequisite of life. Among self-assembling proteins that lead to extremely stable structures are collagens, keratins, and silks.[24,25] These proteins form exceptionally strong polymer networks, which derive their strength mainly from hydrogen bonding between protein chains.[26,27] Among these protein polymers, spider silk reveals the most outstanding mechanical properties.[24–31] Spider silk is further known to only illicit a minimal allergenic and immunological response when implanted.

Of the different types of spider silks, draglines from the garden cross spider *Araneus diadematus* are among the most intensely studied.[26,27] The dragline silk fibers are formed from two different proteins, ADF-3 and ADF-4 (the name is derived from Araneus Diadematus Fibroin). Recently, we have developed a gene-engineering technique that allows for the recombinant production of spider-silk proteins engineered for

[*] Dr. T. Scheibel, Dr. D. Huemmerich
Lehrstuhl für Biotechnologie
Technische Universität München
Lichtenbergstr. 4, 85747 Garching (Germany)
E-mail: thomas.scheibel@ch.tum.de
Prof. A. R. Bausch, Dr. K. D. Hermanson
Lehrstuhl für Biophysik E22
Technische Universität München
James-Franck-Str., 85747 Garching (Germany)
E-mail: abausch@ph.tum.de

[**] The authors would like to thank Hendrik Dietz for his help with the AFM measurements, Gerrit Vliegenthart and Gerhard Gompper for useful discussions, and Markus Harasim. The work was supported by the DFG (BA 2029/5 (A.R.B.) and SCHE 603/4-1 (T.S.)) and the support of the Nanosystems Initiative Munich (NIM) is gratefully acknowledged. K.D.H. was supported by the Alexander von Humboldt Foundation.

high-yield production in bacteria.[32] One protein produced through this technique, C_{16}, mimics ADF-4 by containing 16 of the ADF-4 consensus repeat units. C_{16} can not only be assembled into fibers similar to those produced in Nature, but it can also be assembled into other structures such as thin films or hydrogels.[33–35]

Here we show that the engineered spider-silk protein C_{16} can be assembled at an oil/water interface to form a microcapsule with high mechanical stability. For the assembly of the microcapsules, an aqueous solution of C_{16} with concentrations between 1–6 mg mL^{-1} was emulsified in toluene. Because of the amphiphilic nature of C_{16},[36,37] it adsorbed quickly at the interface. After adsorption, the protein immediately assembled and formed a film at the surface of the water droplets, encapsulating its contents (Fig. 1). During the self-assembly process C_{16} underwent a conformational change from a structure that was mainly random coil to one that was β-sheet rich. For this procedure any oil which promotes protein adsorption and conformational change can be used in place of toluene. Using the same methodology, other types of oils, including a variety of alkanes, silicon oils, and aromatics, have been tested. Among the oils tested, aromatic oils appeared to promote protein assembly and microcapsule formation the best.

Previous investigations of proteins at interfaces have shown that proteins will often adsorb and denature at an interface to form a film.[38,39] These studies have shown that the rate of film formation for most proteins is slow, taking from minutes to hours, since several processes have to take place in a defined order: i) protein adsorption, ii) protein unfolding, and iii) protein refolding and assembly.[39] The adsorption is entropic in origin and is largely driven by amino acid residues displacing water from the interfacial region.[38]

The mechanism of silk-protein assembly is thought to be similar to the adsorption of other proteins at surfaces (Fig. 1). However, unlike other proteins C_{16} is intrinsically unfolded, with all typical characteristics of an intrinsically unfolded protein,[32] and therefore no protein unfolding has to take place at the interface. In contrast to the slow kinetics that have been observed with other proteins the silk microcapsules form rapidly, with the whole adsorption and assembly process taking less than 30 seconds. This rapid process is partially a result of the protein concentration in the initial solution and of the small droplet size, both of which promote rapid diffusion of the protein to the interface and, subsequently, a fast adsorption rate. If it assumed that there is a negligible energy barrier to protein adsorption, the adsorption rate ($d\Gamma/dt$) can be related to the droplet radius, R, and initial protein concentration, c_0, through the diffusion coefficient, D, by solving Fick's law of diffusion for a spherical droplet initially at a uniform protein concentration. In this case the general solution to Fick's law is obtained by using the method of separation of variables and by summing over a number of particular solutions:

$$\Gamma(t) = \frac{c_o R}{3}\left(1 - \sum_{n=1}^{\infty} \frac{6}{n^2\pi^2}\exp\left(-\pi^2 n^2 \frac{Dt}{R^2}\right)\right) \quad (1)$$

where Γ is the protein concentration at the droplet interface. For droplets with $R = 5$ μm and protein concentrations of $c_0 = 3$ mg mL^{-1} this equation predicts that 99 % of the protein will adsorb in less than 0.5 seconds, assuming a diffusion coefficient of 1×10^{-10} m^2 s^{-1}.[39] This prediction slightly underestimates the total adsorption time because the energy barrier to adsorption is most likely not zero. However, with other proteins similar equations have been shown to describe the initial 70 % of protein adsorption to an oil/water interface, and the total adsorption time has been shown to be of the same order of magnitude.[39,40]

Once the silk microcapsules had formed at the interface, two different methods were used to transfer the C_{16} microcapsules into a continuous phase solution. In the first method, an aqueous sublayer was added below the toluene, and the microcapsules were transferred through centrifugation. In the second method, the two-phase emulsion was transformed into a single-phase solution by adding ethanol to solubilize the water and the toluene. Both transfer methods resulted in stable C_{16} microcapsules that encapsulated the contents of the initial water droplet. The entire process takes less than 30 seconds, making it a fast and efficient method for the encapsulation of active ingredients. The size of the microcapsules can be conveniently controlled by adjusting the emulsion droplet size through changes in the emulsion shear rate. As a result, silk capsules with diameters between 1 and 30 μm can be easily produced.

The final C_{16} assembly exhibits the characteristics of an extremely thin protein film (Fig. 2A). Scanning electron microscopy images of the microcapsules demonstrate that the microcapsules are

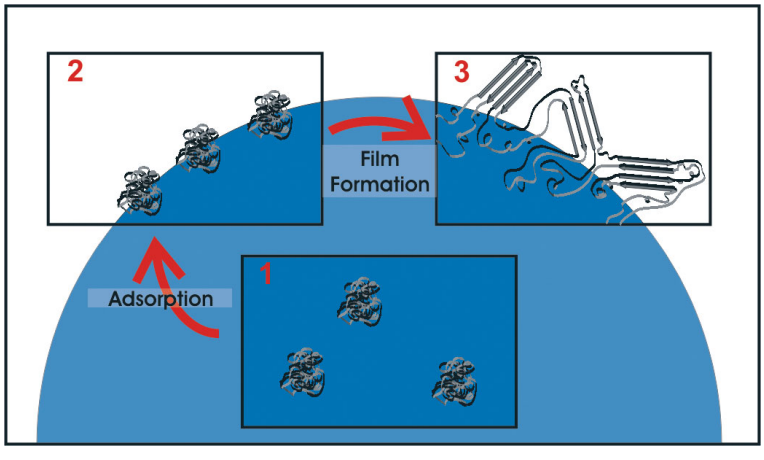

Figure 1. Schematic illustration of the C_{16} assembly process at the interface between water and toluene. 1) C_{16} is first soluble in the water droplet. 2) Subsequently, C_{16} adsorbs on the droplet interface. 3) At the interface, the silk protein self-assembles into a nanometer-thin film.

ADVANCED MATERIALS

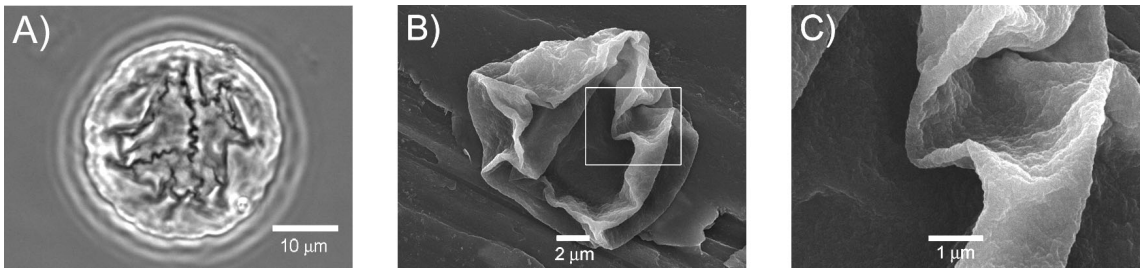

Figure 2. Scanning electron microscopy images of dried microcapsules. A) Microcapsule after centrifugation into dextran solution. Folds in the capsule are caused by high outside osmotic pressure. B) Dried microcapsule. C) Higher-magnification image of the boxed area in (B).

hollow, contain no visible defects, and have membranes that are very thin (Fig. 2B and C). It is apparent from the SEM images that the membrane is no larger than 50 nm, and most likely much less because the SEM technique is only capable of showing a fold in the membrane. The thin membranes observed by SEM are not surprising, considering the concentration of the silk protein suspension and the size of the encapsulated emulsion droplet. At the formation conditions ($c = 3.5$ mg mL^{-1}, $r = 5$ μm) a mass balance shows that the membrane thickness cannot be larger than 6 nm. This maximum thickness assumes that all of the silk protein adsorbs to the surface of the emulsion droplet, and that the polymer film has a density of 1 g mL^{-1}.

Unlike intrinsically unstructured soluble C_{16}, the assembled protein has a β-sheet-rich conformation. The change in C_{16} conformation upon assembly was observed by using IR spectroscopy. Initially, C_{16} in D_2O adsorbed at 1645 cm^{-1}, which is characteristic of proteins with a random coil structure (Fig. 3). After microcapsule formation two shoulders in the adsorption spectra emerge, indicating a change in the secondary structure of C_{16}. Deconvolution of the spectra, by the method proposed by Byler and Susi,[41] reveals the contribution of four Gaussian peaks at 1621, 1642, 1661, and 1683 cm^{-1}. These peaks are assigned to β-sheets, random coil structures, and β-turns (two peaks), respectively. Peaks at these locations are also observed in natural spider and silk worm silk, and are also thought to result from the adsorption by β-sheets and random coil structures.[42,43] From the deconvolution, it is determined that 32 % of the C_{16} structure within the final microcapsules is β-sheet, 40 % is β-turn and 28 % is random coil. Previous studies of structures formed by recombinant proteins in solvent-cast films have shown that the exact composition of the formed films is highly dependent on the numbers of each structural motif used to form the protein, but that the peak location for the formed structures is invariant.[26,32–34]

An important feature of the employed microencapsulation technique is the ease by which water-soluble molecules can be encapsulated. To encapsulate molecules they must first be solubilized in the initial silk protein suspension. When emulsified, the silk protein will adsorb onto the droplet surface and encapsulate the contents of the initial water droplet. Figure 4

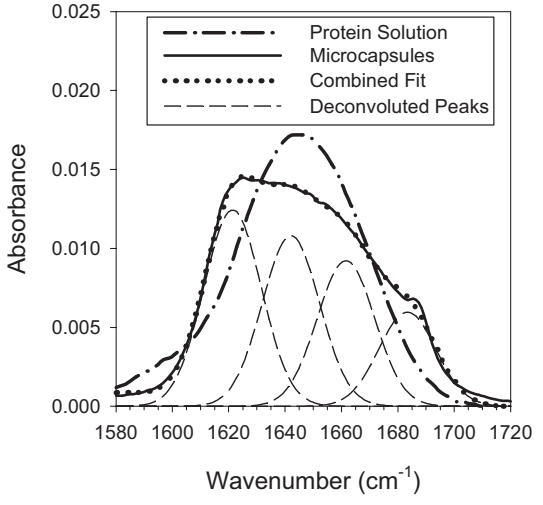

Figure 3. IR spectra in D_2O before (dashed–dotted line) and after (solid line) microcapsule formation. The shift in the spectra indicates the formation of β-sheets. Deconvolution and Gaussian fit of the microcapsule IR spectra reveals four peaks. Deconvoluted peaks are present at 1621, 1642, 1661, and 1683 cm^{-1}, and are assigned to β-sheets, random coil structures, and β-turns (two peaks), respectively.

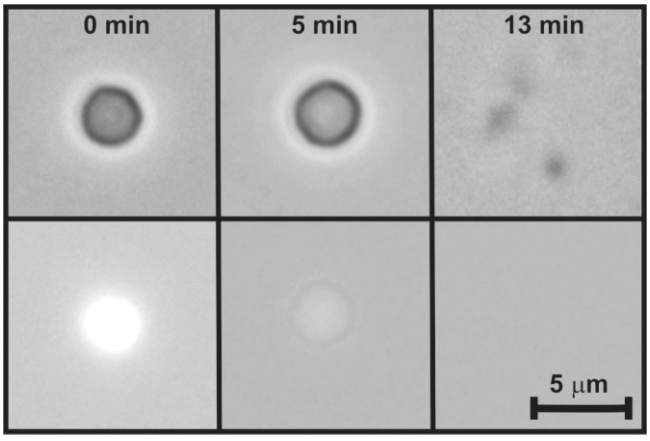

Figure 4. Proteinase K digestion of C_{16} microcapsules encapsulating FITC-labeled dextran. Top row: phase-contrast image. Bottom row: fluorescent image. As indicated by the loss of fluorescence, dextran is released shortly after addition of proteinase K. Complete digestion of microcapsules occurs after (13 ± 1) min. 100 μg mL^{-1} proteinase K, 0.1 % sodium dodecyl sulfate, 37 °C, 0.5 % encapsulated 40 kDa FITC–dextran.

(0 min) shows the encapsulation of fluorescently labeled dextran with a molecular weight of 40 kDa.

The C_{16} capsules have been observed to be impermeable to large dextrans, while low-molecular-weight molecules, such as the fluorescent molecule fluorescein, freely diffuse across the membrane. When polydisperse, low-molecular-weight, fluorescently labeled dextran ($M_w = 38$ kDa) is added to the outside of the silk microcapsules only a fraction of the dextran permeates the microcapsules (Fig. 5). A similar partial permeation of fluorescently labeled dextran has been previously observed in other capsules that contained polyelectrolyte.[44,45] In these experiments, 0.1 M NaCl was added to the silk microcapsule suspension to eliminate any charge effects resulting from trapped unabsorbed spider silk. The previously observed partial permeation resulted from the entrapped polyelectrolyte that produced a Donnan effect, and was very sensitive to the concentration of other ions present. Unlike the previously observed capsules, the partial permeation through the silk microcapsules is not observed for charged fluorescein molecules, demonstrating that this partial permeation is not caused by a Donnan effect. In the case shown here, the partial dextran permeation is a result of the permeation of the fraction by the dextran with a molecular weight lower than the cut-off of the membrane. By measuring the amount of dextran that permeated the membrane of 52 microcapsules from 15 different samples and comparing this to the dextran molecular weight distribution, the average molecular weight cut-off was measured to be 27 kDa ($r_g \approx 53$ Å[46]).

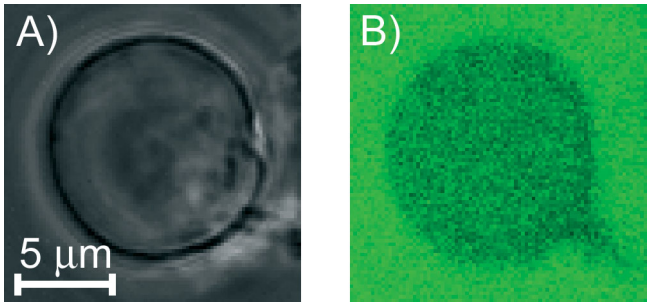

Figure 5. Permeability of polydisperse 38 kDa FITC-labeled dextran of one of the 52 microcapsules measured. A) Brightfield image of a microcapsule. B) Partial permeation of FITC–dextran measured by laser scanning confocal microscopy.

Not surprisingly, spider-silk microcapsules exhibit exceptional strength and tenacity. As a result, high concentrations of an active ingredient can be encapsulated without the microcapsule rupturing from osmotic stress. The stability was affirmed by the successful encapsulation of 1 MDa poly(sodium styrene sulfonate) at concentrations that exceed an osmotic stress of 10^7 Pa (data not shown). The microcapsules were also observed to be highly elastic. When probed with a microneedle, the microcapsules can be deformed but immediately recover their initial shape upon removal of the microneedle. The mechanical properties of the microcapsules were further measured by compression with an atomic force microscope. At small deformations, the relationship between the applied force, f, and the resultant deformation, ε, is described by

$$f \propto E h^2 \varepsilon / \sqrt{12(1-\sigma^2)} \quad (2)$$

where h is the membrane thickness, E is the Young's modulus, σ is the Poisson ratio, and the prefactor is a constant of an order of one.[47–49] By using the maximum capsule wall thickness calculated from the initial concentration of silk monomer used and by assuming a Poisson ratio of 0.5, the microcapsules were determined to have a Young's modulus in the range of 0.7–3.6 GPa. This value compares well to the Young's modulus of natural *Araneus diadematus* dragline silk of 10 GPa.[31] The capsules also demonstrate excellent chemical stability. The addition of protein denaturants such as 2 % sodium dodecylsulfate (SDS) and 8 M urea has no effect on capsule integrity. The microcapsules were observed to be stable under these conditions for weeks.

While the capsules are stable against several chemical denaturants, release of the contents can be triggered by enzymatic degradation of the employed C_{16} protein. Enzymatic triggered release of contents, such as fluorescein isothiocyanate (FITC) labeled dextran, was demonstrated by using the enzyme Proteinase K (Fig. 4). As indicated by the loss of fluorescence shortly after the addition of Proteinase K, the integrity of the microcapsule membrane is destroyed and the dextran is released. After release of the dextran, the enzyme continues to digest the microcapsule until complete digestion occurs at (13 ± 1) min.

Strikingly, the release mechanism can be modified, because enzymatic digestion of the microcapsules is prevented by chemically cross-linking C_{16} through photoinitiated oxidation with ammonium peroxodisufate (APS) and tris(2,2′-bipyridyl) dichlororuthenium(II) (Rubpy).[50] To chemically crosslink the C_{16}, 10 mM APS and 100 mM Rubpy are added to the centrifuged solution, and the reaction is photoinitiated by exposing the mixture to light from a tungsten lamp for five minutes. This cross-linking renders the C_{16} microcapsules stable against treatment with Proteinase K. After crosslinking, the addition of 100 μM Proteinase K to the crosslinked microcapsules has no effect on capsule integrity, even after incubation for one hour at 37 °C. This behavior is markedly different from the noncrosslinked microcapsules, which release the encapsulated dextran almost immediately under the same conditions. Because the properties of these microcapsules can be easily controlled, they can be adapted for a wide range of applications. Using the protein-engineering approach from which C_{16} is generated[26,32,34] the microcapsules can be even further tailored to degrade the C_{16} membrane in response to tissue-specific enzymes by incorporating specific amino acid sequences. Specific release mechanisms, therefore, can be easily engineered into the spider silk microcapsules.

The presented microcapsules, made from spider-silk proteins, introduce a new class of materials made from engineered proteins. Self-assembly of the proteins at an emulsion

ADVANCED MATERIALS

interface leads to the formation of a thin polymer shell that meets the key requirements of encapsulation devices for the controlled encapsulation and release of active ingredients. These microcapsules can be used to encapsulate any small active ingredient, provided that the active ingredient does not impede the adsorption of the silk and/or that the encapsulation process does not alter the ingredient. The modular architecture and simplicity of the spider-silk proteins will make it possible to incorporate highly specific functionalities into the microcapsules, which makes them very promising for a wide range of applications, from drug delivery and flavor encapsulation to microreactors. The ease of encapsulation and ability to produce the recombinant silk protein in large quantities makes this technique a practical encapsulation method.

Experimental

Dragline silk protein ADF-4 from the garden spider *Araneus diadematus* was used as template for the spider-silk construct C_{16}, engineered for bacterial expression [26,32]. The repetitive part of ADF-4 is generally composed of a single conserved repeat unit displaying only slight variations. These variations were combined from a one consensus module termed C (GSSAAAAAAAASGPGGYGPENQGPSGPGGYGPGGP), which was oligomerized to obtain the repetitive protein C_{16}. The resulting C_{16} protein had a molecular mass of 48 kDa [32].

The C_{16} silk gene was expressed in the *Escherichia coli* strain BLR [DE3] (Novagen). Cells were grown at 37 °C in LB medium to an OD600 = 0.5. Before induction with 1 mM isopropyl-*β*-D-thiogalactoside (IPTG), cells were shifted to 25 °C. Cells were harvested after 3–4 h of induction. C_{16} protein was purified, and protein identity and purity was assessed as described by Huemmerich et al. [32].

The protein solution from which the microcapsules were formed was prepared by first dissolving lyophilized C_{16} silk protein at a concentration of 10 mg mL^{-1} in 6 M guanidine thiocyanate. The protein solution was then cooled to 4 °C, and the protein solution was dialyzed against 10 mM tris(hydroxymethyl) aminomethane, pH 8.0, overnight by using dialysis tubing from Carl Roth GmbH & Co. with a molecular weight cut-off of 14 kDa. Any protein that was not dispersed was removed by centrifuging the dialyzed solution for 30 min at 100 000 *g* at 4 °C. The final protein concentration was determined by UV adsorption. The recombinant protein has an extinction coefficient of 46 400 M^{-1} cm^{-1} at a wavelength of 276 nm.

The microcapsules were formed by emulsifying 5 μL of dialyzed protein solution in 300 μL toluene for 90 s. Silk microcapsules were formed using protein solutions with concentrations ranging from 1 to 6 mg mL^{-1} and with emulsification times as short as 30 s. The size of the microcapsules depended on the size of the emulsion droplets. Once formed the polymer shells surrounding the emulsion droplets were transferred from the two-phase emulsion into a one-phase solution. Two different methods were shown to be effective in transferring the polymer shells. In the first method, 300 μL of water was added to the toluene to form an aqueous sublayer. The polymer shells surrounding the water droplets were then centrifuged from the toluene layer into the aqueous sublayer at a force of 100 *g* for 4 min. In the second method, a single-phase solution was formed by adding 300 μL of ethanol (95 %) to the two-phase emulsion to solubilize the toluene and water. After using either method to transfer the microcapsules to a single-phase solution, microcapsules were observed with a Zeiss Axiovert 200M optical microscope.

The integrity of the centrifuged microcapsules was verified by adding 0.5 wt % FITC-labeled 40 kDa dextran (Sigma–Aldrich) to the protein solution prior to emulsification. After emulsification and centrifugation, the formed microcapsules continued to fluoresce, proving that the polymer shells of these structures did not tear during centrifugation. The fluorescence provided by the encapsulated FITC-labeled dextran was stable for at least 20 days. Without the addition of FITC-labeled dextran no fluorescence was observed. Fluorescence microscopy was also performed on a Zeiss Axiovert 200M microscope.

SEM images of the microcapsules were obtained by drying a solution after centrifugation on an unpolished aluminum SEM stud, sputtering with gold and examining with a Jeol JSM-5900 microscope operated at an acceleration voltage of 15 kV.

Microcapsule permeability was measured by adding 38 kDa FITC-labeled dextran at a concentration of 0.67 % to the outside of the aqueous microcapsule dispersion. Before observation with a confocal microscope the dextran concentration in the microcapsules was allowed 12 h at room temperature to come to equilibrium. Confocal microscopy (Zeiss LSM 510) was used for measuring the dextran concentration inside and outside of the microcapsules. To determine the amount of dextran that permeated the capsules, the measured fluorescent intensity at the center of the capsules was compared to the fluorescent intensity of the surrounding medium at the same focal depth. The dextran molecular weight that permeated the capsules was determined by comparing the fluorescence measured by confocal microscopy with the cumulative fluorescence molecular weight distribution as measured by gel permeation chromatography (GPC).

An Agilent 1100 GPC instrument with both ultraviolet and refractive index detectors was used to measure the FITC-labeled dextran molecular weight. The instrument was equipped with one precolumn (Polymer Standards Suprema SUA080520) and three analytical columns (Polymer Standards Suprema SUA0830101E2, SUA0830101E3, and SUA0830103E3) that allowed the instrument to separate polymers with sizes between 100 Da and 1.6×10^6 Da. The GPC molecular weight calibration was done using 14 dextran calibration standards ranging in molecular weight from 180 Da to 4.01×10^4 Da.

For the GPC measurements, 3.0 g L^{-1} of the FITC-labeled dextran was dissolved in 0.1 M $NaNO_3$ overnight. The sample solution was filtered through a 1.0 μm filter to remove any undissolved dextran and dust particles, and then eluted through the column with 0.1 M $NaNO_3$ at a flow rate of 1.0 mL min^{-1}. The dextran molecular weight was measured using a refractive index detector and the amount of fluorescent labeling at each molecular weight was determined by measuring FITC adsorption at 488 nm.

IR measurements were preformed using a Bruker IFS 66/s spectrometer. For measurements performed on soluble C_{16} a fixed path length flow cell with CaF_2 windows (Bruker AquaSpec) was used. The cell was first rinsed with 10 mM Tris buffer in D_2O with a pH of 8.0. First, a background spectrum of the Tris buffer was obtained. A 3 mg mL^{-1} sample of C_{16} protein dissolved in 10 mM Tris buffer in D_2O was then injected into the sample cell, and the protein spectrum was obtained after subtraction of the background. Spectra of the final microcapsules were obtained using an infrared microscope (Bruker IRscope). Microcapsules were first prepared from C_{16} dissolved in 10 mM Tris D_2O buffer. After emulsification in Toluene and centrifugation into D_2O, the IR spectra of individual microcapsules in a CaF_2 microscopy slide were taken using a 36× objective, and the background spectra were obtained from sample points where no microcapsules were present.

Using a custom-built atomic force microscope, AFM measurements were made on microcapsules in an aqueous suspension. Small deformations to the microcapsules were applied using a 35 μm glass sphere attached to an AFM cantilever with a spring constant of 10 pN nm^{-1} (BioLevers, Olympus, Tokyo).

Received: November 27, 2006
Revised: January 10, 2007
Published online: June 20, 2007

[1] F. Caruso, R. A. Caruso, H. Mohwald, *Science* **1998**, *282*, 1111.
[2] A. D. Dinsmore, M. F. Hsu, M. G. Nikolaides, M. Marquez, A. R. Bausch, D. A. Weitz, *Science* **2002**, *298*, 1006.
[3] O. D. Velev, K. Furusawa, K. Nagayama, *Langmuir* **1996**, *12*, 2374.

[4] B. M. Discher, Y. Y. Won, D. S. Ege, J. C. M. Lee, F. S. Bates, D. E. Discher, D. A. Hammer, *Science* **1999**, *284*, 1143.
[5] S. Santoso, W. Hwang, H. Hartman, S. G. Zhang, *Nano Lett.* **2002**, *2*, 687.
[6] H. Kukula, H. Schlaad, M. Antonietti, S. Forster, *J. Am. Chem. Soc.* **2002**, *124*, 1658.
[7] M. S. Wong, J. N. Cha, K. S. Choi, T. J. Deming, G. D. Stucky, *Nano Lett.* **2002**, *2*, 583.
[8] J. B. Li, H. Mohwald, Z. H. An, G. Lu, *Soft Matter* **2005**, *1*, 259.
[9] A. M. Yu, Y. J. Wang, E. Barlow, F. Caruso, *Adv. Mater.* **2005**, *17*, 1737.
[10] S. Vauthey, S. Santoso, H. Y. Gong, N. Watson, S. G. Zhang, *Proc. Natl. Acad. Sci. USA* **2002**, *99*, 5355.
[11] G. A. Silva, C. Czeisler, K. L. Niece, E. Beniash, D. A. Harrington, J. A. Kessler, S. I. Stupp, *Science* **2004**, *303*, 1352.
[12] S. G. Zhang, *Nat. Biotechnol.* **2003**, *21*, 1171.
[13] Y. C. Yu, P. Berndt, M. Tirrell, G. B. Fields, *J. Am. Chem. Soc.* **1996**, *118*, 12 515.
[14] A. Mahler, M. Reches, M. Rechter, S. Cohen, E. Gazit, *Adv. Mater.* **2006**, *18*, 1365.
[15] M. G. Ryadnov, D. N. Woolfson, *Nat. Mater.* **2003**, *2*, 329.
[16] D. W. Urry, T. Hugel, M. Seitz, H. E. Gaub, L. Sheiba, J. Dea, J. Xu, T. Parker, *Philos. Trans. R. Soc., B* **2002**, *357*, 169.
[17] D. W. Urry, *J. Phys. Chem. B* **1997**, *101*, 11 007.
[18] A. Junger, D. Kaufmann, T. Scheibel, R. Weberskirch, *Macromol. Biosci.* **2005**, *5*, 494.
[19] S. Winkler, S. Szela, P. Avtges, R. Valluzzi, D. A. Kirschner, D. Kaplan, *Int. J. Biol. Macromol.* **1999**, *24*, 265.
[20] R. G. Lebaron, K. A. Athanasiou, *Tissue Eng.* **2000**, *6*, 85.
[21] J. L. West, J. A. Hubbell, *Macromolecules* **1999**, *32*, 241.
[22] G. Lu, Z. H. An, J. B. Li, *Biochem. Biophys. Res. Commun.* **2004**, *315*, 224.
[23] Z. H. An, G. Lu, H. Mohwald, J. B. Li, *Chem. Eur. J.* **2004**, *10*, 5848.
[24] J. Gosline, M. Lillie, E. Carrington, P. Guerette, C. Ortlepp, K. Savage, *Philos. Trans. R. Soc., B* **2002**, *357*, 121.
[25] T. Scheibel, L. Serpell, in *Protein Folding Handbook*, Vol. 2 (Eds: J. Buchner, T. Kiefhaber), Wiley-VCH, Weinheim, Germany **2005**, p. 193.
[26] T. Scheibel, *Microb. Cell Fact.* **2004**, *3*, 14.
[27] F. Vollrath, *Rev. Mol. Biotechnol.* **2000**, *74*, 67.
[28] M. B. Hinman, J. A. Jones, R. V. Lewis, *Trends Biotechnol.* **2000**, *18*, 374.
[29] S. Winkler, D. L. Kaplan, *Rev. Mol. Biotechnol.* **2000**, *74*, 85.
[30] J. Bai, T. Ma, W. Chu, R. Wang, L. Silva, C. Michal, J.-C. Chiao, M. Chiao, *Biomed. Microdevices* **2006**, *8*, 317.
[31] J. M. Gosline, P. A. Guerette, C. S. Ortlepp, K. N. Savage, *J. Exp. Biol.* **1999**, *202*, 3295.
[32] D. Huemmerich, C. W. Helsen, S. Quedzuweit, J. Oschmann, R. Rudolph, T. Scheibel, *Biochemistry* **2004**, *43*, 13 604.
[33] U. Slotta, M. Tammer, F. Kremer, P. Koelsch, T. Scheibel, *Supramol. Chem.* **2006**, *18*, 465.
[34] D. Huemmerich, U. Slotta, T. Scheibel, *Appl. Phys. A* **2006**, *82*, 219.
[35] S. Rammensee, D. Huemmerich, K. D. Hermanson, T. Scheibel, A. R. Bausch, *Appl. Phys. A* **2006**, *82*, 261.
[36] C. W. P. Foo, E. Bini, J. Hensman, D. P. Knight, R. V. Lewis, D. L. Kaplan, *Appl. Phys. A* **2006**, *82*, 223.
[37] J. P. Zbilut, T. Scheibel, D. Huemmerich, C. L. Webber, M. Colafranceschi, A. Giuliani, *Phys. Lett. A* **2005**, *346*, 33.
[38] S. R. Euston, *Curr. Opin. Colloid Interface Sci.* **2004**, *9*, 321.
[39] D. E. Graham, M. C. Phillips, *J. Colloid Interface Sci.* **1979**, *70*, 403.
[40] A. V. Makievski, G. Loglio, J. Kragel, R. Miller, V. B. Fainerman, A. W. Neumann, *J. Phys. Chem. B* **1999**, *103*, 9557.
[41] D. M. Byler, H. Susi, *Biopolymers* **1986**, *25*, 469.
[42] S. Szela, P. Avtges, R. Valluzzi, S. Winkler, D. Wilson, D. Kirschner, D. L. Kaplan, *Biomacromolecules* **2000**, *1*, 534.
[43] H. Teramoto, M. Miyazawa, *Biomacromolecules* **2005**, *6*, 2049.
[44] W. J. Tong, W. F. Dong, C. Y. Gao, H. Mohwald, *J. Phys. Chem. B* **2005**, *109*, 13 159.
[45] W. J. Tong, H. Q. Song, C. Y. Gao, H. Mohwald, *J. Phys. Chem. B* **2006**, *110*, 12 905.
[46] F. R. Senti, N. N. Hellman, N. H. Ludwig, G. E. Babcock, R. Tobin, C. A. Glass, B. L. Lamberts, *J. Polym. Sci.* **1955**, *17*, 527.
[47] F. Dubreuil, N. Elsner, A. Fery, *Eur. Phys. J. E* **2003**, *12*, 215.
[48] L. D. Landau, E. M. Lifschitz, *Elastizitätstheorie*, Vol. 7, Akademie Verlag, Berlin **1991**.
[49] G. A. Vliegenthart, G. Gompper, *Biophys. J.* **2006**, *91*, 834.
[50] D. A. Fancy, T. Kodadek, *Proc. Natl. Acad. Sci. USA* **1999**, *96*, 6020.